Biochemical and Biophysical Research Communications 423 (2012) 832–837

Contents lists available at SciVerse ScienceDirect

Biochemical and Biophysical Research Communications

journal homepage: www.elsevier.com/locate/ybbrc

Aristolochic acid-induced accumulation of methylglyoxal and N^{ε}-(carboxymethyl)lysine: An important and novel pathway in the pathogenic mechanism for aristolochic acid nephropathy

Yi-Chieh Li [a,1], Shin-Han Tsai [b,1], Shih-Ming Chen [a], Ya-Min Chang [c], Tzu-Chuan Huang [a], Yu-Ping Huang [a], Chen-Tien Chang [c], Jen-Ai Lee [a,*]

[a] School of Pharmacy, College of Pharmacy, Taipei Medical University, No. 250 Wuxing St., Taipei 11031, Taiwan, ROC
[b] Department of Emergency Medicine and Critical Care Medicine, Taipei Medical University-Shuang Ho Hospital, No. 291, Zhongzheng Rd., Zhonghe District, New Taipei City 23561, Taiwan, ROC
[c] Department of Food and Nutrition, Providence University, No. 200, Chung Chi Rd., Taichung, Taiwan, ROC

ARTICLE INFO

Article history:
Received 7 June 2012
Available online 16 June 2012

Keywords:
Aristolochic acid
Aristolochic acid nephropathy
Methylglyoxal
Advanced glycation end products
N^{ε}-(carboxymethyl)lysine
Glutathione

ABSTRACT

Aristolochic acid, found in the *Aristolochia* species, causes aristolochic acid nephropathy (AAN) and can develop into renal failure. Methylglyoxal (MGO) is a highly cytotoxic compound generated from the metabolic process of glucose or fatty acids. It binds to proteins and forms N^{ε}-(carboxymethyl)lysine (CML), which contributes to aging and diabetes mellitus complications. However, no relevant literature explores the relationship of MGO and CML with AAN. By injecting AA (10 mg/kg BW) into C3H/He mice for 5 consecutive days, we successfully developed an AAN model and observed tubular atrophy with decreased renal function. Creatinine clearance also decreased from 10.32 ± 0.79 ml/min/kg to 2.19 ± 0.29 ml/min/kg ($p < 0.01$). The concentration of MGO in kidney homogenates increased 12×compared to the control group (from 18.23 ± 8.05 μg/mg of protein to 231.16 ± 17.57 μg/mg of protein, $p < 0.01$), and CML was observed in the renal tubules of the mice by immunohistochemistry. Furthermore, compared to the control group, GSH levels decreased by 0.32×(from 2.46 ± 0.41 μM/μg of protein to 0.78 ± 0.15 μM/μg of protein, $p < 0.01$), whereas intra-renal antioxidant capacity decreased by 0.54×(from 6.82 ± 0.97 U to 3.71 ± 0.25 U; unit is equivalent to μM Trolox/mg of protein, $p < 0.01$). In this study, we found that serious kidney damage induced by AA is related to an increase and accumulation of MGO and CML.

1. Introduction

Aristolochic acid nephropathy (AAN) is a type of progressive interstitial nephropathy that may lead to permanent, irreversible renal failure [1]. In Belgium, researchers reported that a group of patients who took *Aristolochia fangchi* to lose weight later developed renal failure [2]. Traditionally, *Aristolochia* has been used to treat arthritis, infections, inflammations, and tumors [3,4]. It was once inappropriately used as a substitute for *Stephania tetrandra,* which led to Chinese herb nephropathy, later named AAN. Large amounts of aristolochic acid (AA) are found in *Aristolochia*, and AA has also been discovered in other plants. The Food and Drug Administration has advised the population to stop using botanical products containing AA. However, certain products containing AA remain available through online purchasing or because of contamination in herbal remedies [5]. Previously, the pathogenic mechanism for AAN was unclear, but several hypotheses on the mechanism exist; for example, direct cell toxicity [6], ischemia-induced tubular atrophy [7], and epithelial–mesenchymal transition [8]. Besides, antioxidant enzyme dysfunction and mitochondrial damage were observed in rats injected with AA [9].

Methylglyoxal (MGO) is a reactive intermediate metabolic of glycolysis and is also derived from amino acids and acetone [10]. Levels of MGO are elevated in serum and renal tissue in diabetic patients [11]. MGO is a highly cytotoxic compound and both the production and removal of MGO are involved in radical generation [10]. Also, MGO is detoxified through the glyoxalase system, which comprises glyoxalase I and II and uses a catalytic amount of GSH. The MGO also undergoes non-enzyme reactions that rapidly react with protein to form advanced glycation end products (AGEs), such as N^{ε}-(carboxymethyl)lysine (CML). It is considered an indicative marker of diabetes mellitus complications [12].

Abbreviations: AA, aristolochic acid; AAN, aristolochic acid nephropathy; MGO, methylglyoxal; AGEs, advanced glycation end products; CML, N^{ε}-(carboxymethyl)lysine; GSH, glutathione; BUN, blood urea nitrogen; NAG, *N*-acetyl-β-D-glucosaminidase; Ucr, urinary creatinine; i.p., intraperitoneal injection.

* Corresponding author. Fax: +886 2 27361661x6120.
E-mail address: jenai@tmu.edu.tw (J.-A. Lee).

[1] These authors contributed equally to this work.

0006-291X/$ - see front matter © 2012 Elsevier Inc. All rights reserved.
http://dx.doi.org/10.1016/j.bbrc.2012.06.049

Lou et al. showed that AA administered to rats caused the accumulation of fat droplets in renal tubular cells and systemic disturbance of free fatty acid [13]. Because fatty acid is a source of MGO [10], we were doubtful as to whether MGO also increased in the kidneys of AA mice. Moreover, Yu et al. discovered that exposing AA to human cells could induce oxidative DNA damage associated with GSH depletion [14]. GSH is a necessary component in metabolized MGO. Exposing AA to human promyelocytic leukemia cells (HL-60) caused GSH depletion, implying that MGO could be mass produced when cells are incubated with AA. Although MGO is such an important cytotoxic constituent, somehow no paper has yet referred to the relationship between MGO and AAN. The purpose of this study was to determine if a change occurs in MGO levels in the AAN model.

This study analyzed intra-renal MGO and CML levels in an AAN model as well as the relationship of the intra-renal GSH level and oxidative stress at the same time.

2. Materials and methods

2.1. Chemicals

Citric acid, bovine serum album (BSA), creatinine, paraformaldehyde, sodium bisulfate, sodium heparin, MGO (40% aqueous solution), AA, sodium hydroxide (NaOH), ammonium chloride, 5,6-Diamino-2,4-dihydroxy-pyrimidine, xylene, and CML antibody were purchased from Sigma–Aldrich Fine Chemicals Inc. (St. Louis, MO, USA). An oxygen radical antioxidant capacity activity assay kit was obtained from Cell Biolabs Inc. (San Diego, CA, USA). A Bio-Rad protein assay kit was purchased from Bio-Rad (Richmond, CA, USA). Acetonitrile (ACN) was purchased from Merck (Darmstadt, Germany). A microalbumin kit was purchased from Goodbiotech (Taichung, Taiwan). A GSH assay kit was purchased from Cayman Chemical (MI, USA).

2.2. Animal treatment and sample preparation

Six-week-old female C3H/He mice were purchased from the National Laboratory Animal Breeding and Research Center (Taipei, Taiwan). All animals received humane care according to guidelines in the *Guidebook for the Care and Use of Laboratory Animals*. The mice were divided into two groups of 8 mice each after 1 week of acclimation. The control group was given 0.1 ml of normal saline by tail vein injection for 5 d (Days 1 through 5). The toxicity group was given 0.1 ml of AA in normal saline (adjust to 10 mg/kg BW) by tail vein injection for 5 d (Days 1 through 5). After given AA for 14 d, both groups were placed in rodent metabolic cages for 24 h for urine collection. Once the experiment was completed, the mice were sacrificed after being anesthetized with pentobarbital (50 mg/kg BW). Blood and kidney samples were collected and stored at −80 °C before use. Kidney samples of 0.25 g were homogenized in 250 μl of cold PBS and centrifuged at 1×10^4g for 10 min at 4 °C. An aliquot of the supernatant was stored at −80 °C for use. Remaining portions of the kidney were fixed in 4% paraformaldehyde solution for later paraffin-embedding.

2.3. Determination of serum and urinary creatinine

Serum and urinary creatinine were determined through HPLC. This process has been described in previous studies [15]. Urine diluted to 25×and used 2 mM cimetidine in 10 mM HCl as the internal standard. Analyzed by HPLC using a Capcell Pak C18 column (25 cm×0.46 cm ID, 5 μm particle size; Shiseido, Tokyo, Japan) and monitored at 234 nm. The mobile phase was composed of ACN and 100 mM of a sodium dihydrogen PBS containing 30 mM sodium lauryl sulfate adjusted to pH 3.0 with hydrochloric acid (36/60, v/v). The flow rate was 0.8 ml/min.

2.4. Determination of blood urea nitrogen (BUN) concentration

The concentration of BUN was determined with an urease assay kit, in which urea was hydrolyzed into ammonia and carbon dioxide using urease. Decreasing levels of NADH were detected by taking readings at A340 nm during the glutamate dehydrogenase catalysis of ammonia and α-ketoglutaric acid into L-glutamic acid [16].

2.5. Determination of N-acetyl-β-D-glucosaminidase (NAG)

Urinary NAG was determined according to Leaback and Walker. The NAG reacted with 4U-methylumbelliferyl-*N*-acetyl-β-glucosaminide (4-MU-NAG) in a 0.15 M glycine buffer (pH 10.3). Fluorescence release was then quantified as a concentration of NAG [17].

2.6. Microalbumin and urine protein

Microalbumin was determined using a commercial kit that employed immunoturbidimetric methods. After conditioning the sample with a Tris buffer, an anti-albumin antibody was added. The sample was incubated for 10 min and then analyzed at 405 nm.

Urine protein was quantified using a Bio-Rad protein assay kit with bovine serum albumin (BSA) as the standard. The absorbance wave of the protein was measured at 595 nm and the concentration was calculated from the BSA standard curve.

2.7. Determination of MGO concentration in kidney samples

Kidney homogenates were stored in the dark at −80 °C. A 0.5 M ammonium chloride buffer (pH 10.0) was added to create an alkaline environment. The derivatizing reagent used was 5,6-Diamino-2,4-dihydroxy-pyrimidine (DDP). After incubation for 30 min at 60 °C, the derivatization reaction was stopped with 0.01 M citric acid (pH 6.0). HPLC analysis was performed on an ODS column (Biosil, 250 mm×4.6 mm ID; 5 μm particle size; Biosil Chemical Co. Ltd., Taipei, Taiwan) at 33 °C. The compounds were separated isocratically using a mobile phase composed of a mixture of ACN and 0.01 M citric acid buffer adjusted to a pH level of 6.0 with NaOH (3/97, v/v).

The flow rate was 0.7 ml/min, the injection volume was 50 μl, and eluted fractions were detected at Ex/Em = 330/500 nm. The MGO standard was used to calculate MGO concentrations in the samples [18].

2.8. Immunohistochemistry

Mouse kidneys were fixed with 4% paraformaldehyde for 2 d, dehydrated with different concentrations of sucrose, and embedded in paraffin. Paraffin sections of 5 μm thickness were used for an immunohistochemistry study to determine the localization and levels of CML. After blocking endogenous peroxidase activity by using 0.3% H_2O_2 for 30 min, CML antibody was diluted 50× to incubate O/N and then reacted for 1 h with goat anti-rabbit IgG conjugated with a peroxidase-labeled second antibody diluted 250×. Peroxidase activity was visualized using a hematoxylin stain. The first antibody was deleted to form the negative control (data not shown).

2.9. Determination of GSH concentration in kidney samples

GSH was measured with the GSH assay kit, which used the sulfhydryl group of GSH reactants with DTNB (5,5′-dithio-bis-(2-nitrobenzoic acid)) and produced yellow 5-thio-2-nitrobenzoic acid (TNB). In brief, tissue homogenates were deproteinized and added to the prepared cocktail by mixing the following reagents: MES Buffer (0.2 M 2-(N-morpholino)ethanesulfonic acid, 0.05 M phosphate, and 1 mM EDTA, pH 6.0), cofactor mixture ($NAPH^+$ and glucose-6-phosphate), GSH reductase and glucose-6-phosphate dehydrogenase, and DTNB. The cocktail was then incubated in the dark, and the absorbance was measured at 405 nm at 5 min intervals for 30 min (totaling 6 measurements). The GSSG was used as the standard to calculate GSH concentration in the kidney [19].

2.10. Antioxidant assay

Antioxidant activity was estimated using an oxygen radical antioxidant capacity assay. The homogenates was diluted 100×prior to assay. Samples were incubated with a fluorescent probe in a 96-well plate for 30 min at 37 °C. 2,2′-Azobis (2-amidinopropane) hydrochloride (AAPH) was added as a free radical initiator. Trolox™ was used as a standard and diluted to 50, 30, 20, 10, 5, 2.5, and 0 μM in 50% acetone. Fluorescence (Ex, 480 nm; Em, 520 nm) was recorded every 5 min for 60 min. The fluorescence decay rate was calculated using the area under the curve (AUC) and compared with the standard. The antioxidant activity of the kidney was also corrected using protein assay.

2.11. Statistical analysis

All data are expressed as the mean ± SEM, and differences between each group were analyzed using two-tailed Student's *t* test. A *p*-value of <0.01 was considered statistically significant.

3. Results

3.1. Successfully induced AAN model: renal function determination

Compared to control mice, mice in the AA group showed significantly increased levels of urinary protein (24.90 ± 2.41 (mg/dl)/Ucr (mg/dl) *vs* 8.40 ± 1.09 (mg/dl)/Ucr (mg/dl), $p < 0.01$). Microalbumin also increased significantly in mice injected with AA (31.39 ± 2.49 (mg/dl)/Ucr (mg/dl) *vs* 0.47 ± 0.07 (mg/dl)/Ucr (mg/dl), $p < 0.01$). Urinary creatinine levels decreased in AA mice (from 21.67 ± 1.30 (mg/dl)/Ucr (mg/dl) to 8.57 ± 0.42 (mg/dl)/Ucr (mg/dl)), but serum creatinine levels increased (from 0.08 ± 0.00 mg/dl to 0.28 ± 0.02 mg/dl). Creatinine clearance (Ccr), an effective index for expressing the glomerular filtration rate (GFR), was calculated using an equation developed by Hsu and Wana and was found to have decreased from 10.32 ± 0.79 ml/min/kg to 2.19 ± 0.29 ml/min/kg [20]. In addition, BUN increased in mice from 24.25 ± 1.70 mg/dl to 117.9 ± 6.70 mg/dl after AA injection. Levels of NAG, an enzyme highly expressed in renal tubules, increase in urine when tubular cells are damaged. Urinary NAG levels rose from 122.77 ± 7.31 U/Ucr (mg/ dl) to 388.89 ± 18.82 U/Ucr (mg/ dl) ($p < 0.01$) in the AA mice group. All renal function data consistently showed that 5 d of AA injected at a rate of 10 mg/kg/d led to kidney malfunction.

3.2. Effects of AA on MGO

Fig. 1A and B showed the HPLC chromatogram of MGO. The MGO was derivated and demonstrated fluorescence with a retention time of 26 min. After quantification with the standard (the linearity range was from 13 to 1170 μg/l, $R = 0.997$, data not shown), MGO levels in the kidney were determined to be significantly higher in the AA group than in the control group (231.16 ± 17.5 μg/g protein *vs* 18.23 ± 8.05 μg/g protein, $p < 0.01$, Fig. 1C).

3.3. Immunohistological staining of CML

With these MGO data, an immunohistochemical analysis was performed to locate CML in mice kidneys after AA treatment. A faint level of CML staining was detected in the control group, but this level increased in the AA group, especially in the tubule region (Fig. 2B).

3.4. Effect of AA on GSH and the antioxidant capacity in the kidney

After 14 d of completion AA injections, GSH levels in the kidney remained significantly low. Intrarenal GSH levels in the AA group were lower than those in the control group (0.78 ± 0.15 μM/μg of protein *vs* 2.46 ± 0.41 μM/μg of protein, $p < 0.01$) (Fig. 3A).

At the same time, the antioxidant ability of AA mice kidneys was determined to be lower than that of the kidneys in control mice, too (3.71 ± 0.25 *vs* 6.82 ± 0.97 U; unit is equal to μM Trolox/μg protein, $p < 0.01$) (Fig. 3B).

3.5. Hypothetical scheme in which AA induces renal damage

Fig. 4 shows a mechanism for AA-induced kidney injury based on an analysis of findings from injecting mice with AA. Levels of MGO and CML were elevated and caused significant carbonyl stress in AA-injected mice. These elevated levels then provoked oxidative stress, causing GSH depletion and reducing antioxidant capacity.

4. Discussion

Several laboratories develop AA models. After administering Wistar rats with 5 mg/kg/d of AA i.p. 5 d/week for 16 week, Zheng et al. sacrificed these rats at weeks 8, 12, 16, 20, and 24 [21]. They observed that, beginning in week 16, BUN and SCR increased significantly, with the appearance of proximal tubular epithelial cell swelling, luminal narrowing, and epithelial cell necrosis. Debelle et al. employed a low dose (1 mg/kg) and a high dose (10 mg/kg) of AA subcutaneous injection in Wistar rats for 35 d and assessed their renal functions [22]. Data from this study showed that injecting 10 mg/kg of AA (equivalent to a dose 30× that given to an AAN patient) induced renal fibrosis and renal failure. The experiment employed in the Debelle et al. study resulted in the successful design of a short-term AAN model similar to a model for humans [22].

The renal function data collected in our study are consistent with that introduced in the literature review: urine protein levels increased, microalbumin appeared, and proximal tubules were damaged in AA-injected mice. Significant decreases in Ccr levels and increases in BUN levels occurred, and urinary NAG, an enzyme highly expressed in the renal tubules, was confirmed to have increased. By using biopsy and pathological diagnosis, the AAN model of mice was imitated successfully (data not shown).

Although the International Agency for Research on Cancer considers high concentrations of AA a Group 1 carcinogen for humans, herbal medicines with low concentrations of AA (e.g., Xixin) are not restricted completely. Therefore, the occurrence of AAN remains a critical problem [1,23]. However, the pathogenic mechanism of AAN is not completely clear. A few in vitro studies investigated the relationship between AA and oxidative stress. Chen et al. suggested that inhibited renal NQO1 activity suppressed nitro reduction, which is the intermediate metabolic of AA and attenuates its nephrotoxicity [24]. AA can also suppress DNA repair

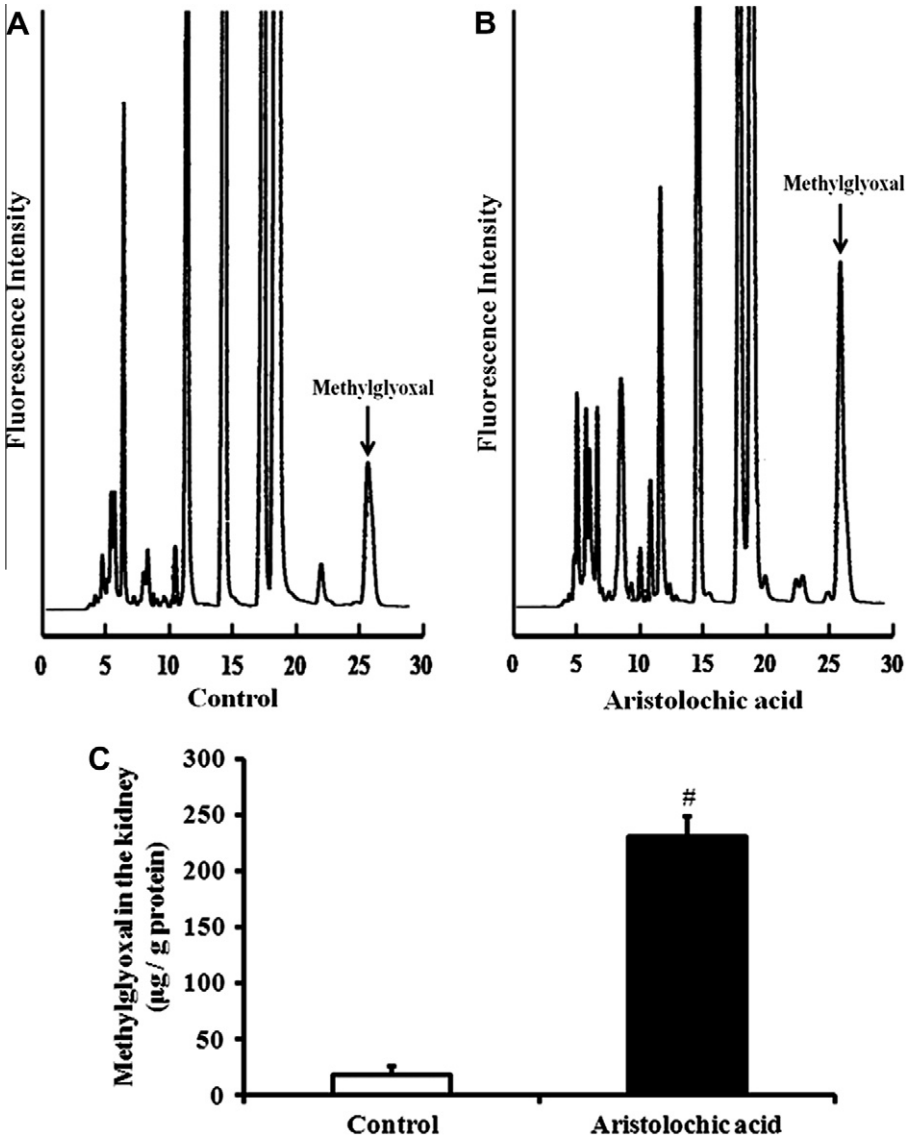

Fig. 1. Effect of AA in the MGO concentration in the mice renal tissues. AA (10 mg/kg/d) was injected (i.v.) for 5 days. MGO was determined by HPLC. Chromatograms of MGO in (A) control and (B) AA 10 mg/kg/d group. MGO was separated at 26 min and normalized by protein concentration. And the quantification of MGO was shown in (C). $^{\#}p < 0.01$ *vs* control group. $n = 6–8$.

and triggers oxidative DNA damage in proximal tubular cells in the human kidney. It also reduces the gene expression of antioxidant enzymes such as superoxide dismutase, GSH reductase, and GSH peroxidase [25]. Yu et al. employed human promyelocytic cells and proximal tubular cells to investigate whether AA induced a dose-dependent increase of reactive oxygen species (ROS) that elevated levels of DNA strand breaks and GSH depletion [14]. Pozdzik et al. discovered that AA could increase oxidative stress, mitochondrial injury, and apoptosis in C3H/He Mice [9]. We also found that antioxidant capacity declines in kidneys affected by AA (from 6.82 ± 0.97 to 3.71 ± 0.25 U; unit is equal to μM Trolox/μg protein) (Fig. 3B), suggesting that oxidative stress is involved in AA toxicity.

However, there is no data about carbonyl stress in AA toxicity. This study analyzed intra-renal MGO and CML levels in an AAN model and the relationship between the intra-renal GSH level and oxidative stress. Following our experiments, the data showed deep connection between carbonyl stress and AAN. Carbonyl stress is represented by MGO and its protein-binding products (AGEs) and may contribute to long-term complications of end-stage renal disease and cardiovascular diseases. [26]. However, even a slightly increased MGO level is enough to cause serious damage to the kidneys over time. In the AAN model, high levels of MGO quickly appeared and resulted in rapid disease development. We observed that the MGO level for the AA-injected mice was 12×that of the control group (Fig. 1C). Because we connected an old-line pathogenic pathway to another new disease, we believe this is an important finding.

We found that serum methylglyoxal did not increase significantly in the kidneys (data not shown) and could be explained by the concentrations of AA. Because organic anion transporters (OATs), which are expressed in proximal tubule cells, are involved in the uptake of AA [27]. AA concentration would greatly increase in proximal tubule cells and trigger MGO and CML accumulation (Figs. 1C and 2B).

In addition, the data show that GSH decreases in the C3H/He AA model (Fig. 3A), a result that is consistent with the in vitro data obtained by Yu et al. [14]. According to the study performed by Yu et al. [14], GSH levels were reduced by 54.9 ± 10.5% after adding 200 μM AAI–HL-60 cells for 30 min. Additional treatment with 5 mM Trion, which may reduce oxidative stress and apoptosis

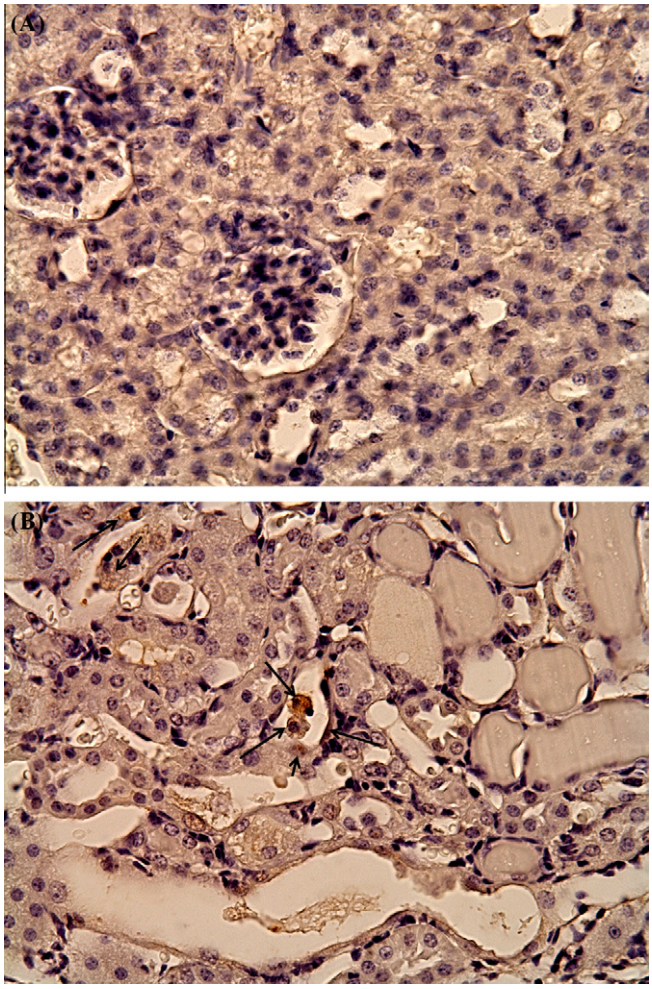

Fig. 2. Immunostaining of CML in mice kidneys after (A) normal saline and (B) AA 10 mg/kg/d, i.v. for 5 days. No CML staining in control kidney but increased CML expression by AA in the tubular cells (arrow) at day 14 in AA-treated mice. Nuclei were counterstained with hematoxylin. Original magnification: 400×.

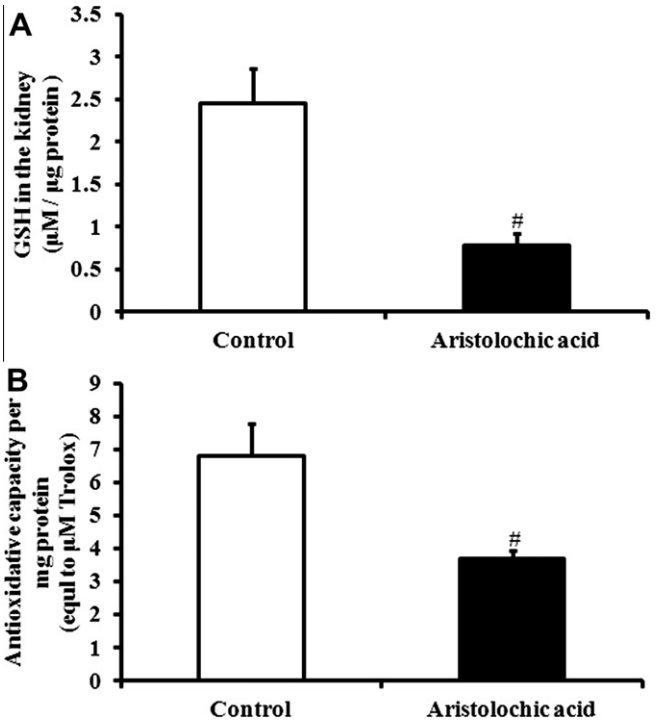

Fig. 3. Effect of AA on GSH concentrations and antioxidant capacity in mice kidneys. (A) GSH concentrations in mice kidneys. (B) The antioxidant capacity in the mice kidneys. The GSH level and antioxidant capacity were determined in the kidney homogenates using DTNB and a fluorescent probe, respectively. The data were corrected using protein assay. $^{\#}p < 0.01$ *vs* control group. $n = 6–8$.

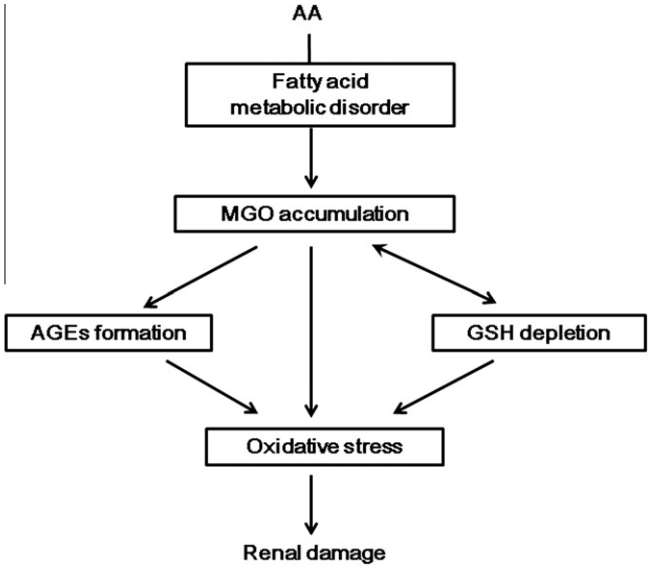

Fig. 4. Hypothetical scheme in which AA induces renal damage. A hypothesis in which AA leads to serious renal damage by elevating carbonyl stress, MGO and CML levels. At the same time reducing GSH levels and antioxidant capacity were also observed.

markers, did not improve GSH levels (57.2 ± 9.8%, compared to the control group); however, additional treatment with 10 mM NAC was determined to possibly reverse a decline in GSH levels (107.2 ± 15.1%, compared to the control group). Their results indicated that, in the pathogenic mechanism of AA, GSH reduction is more important than ROS generation. In our opinion, the reason for decreased antioxidant capacity in the AA model is due to the diminished of GSH in AA mice. And the decreasing GSH level just because the massively MGO accumulation in the kidney.

To date, no standard treatment regimens for AAN exist. In 1993, a group of 12 AAN patients in Belgium with moderate levels of renal failure were treated with prednisolone at 1 mg/kg for 1 month [28], and then with a titer of 0.1 every 2 weeks until the dose was maintained at 0.15 mg/kg. Continued 12-month therapy showed that steroids could inhibit chronic renal interstitial fibrosis caused by AAN; however, half the patients demonstrated side effects because of long-term steroid use. In animal studies, a combined treatment of enalapril for 35 d with 65 d of candesartan did not improve renal function and fibrosis in AAN rats [29]. Clinical doctors remain committed to finding a better regimen to treat AAN. Our discovery of this novel pathogenic pathway, which is the same pathogenic pathway causing diabetes mellitus complications, could introduce MGO-CML control into current AAN therapies and improve treatment efficacy.

Acknowledgments

The authors would like to thank Han, Chuan-Hsiao, and Chang, Chia-hao for their useful advice on experimental techniques. This study was financially supported by the Shuang-Ho Medical Center–Taipei Medical University Joint Research Program (99TMU-SHH-04-4).

References

[1] F.D. Debelle, J.L. Vanherweghem, J.L. Nortier, Aristolochic acid nephropathy: a worldwide problem, Kidney Int. 74 (2008) 158–169.

[2] J.L. Vanherweghem, M. Depierreux, C. Tielemans, et al., Rapidly progressive interstitial renal fibrosis in young women: association with slimming regimen including Chinese herbs, Lancet 341 (1993) 387–391.

[3] V.M. Arlt, M. Stiborova, H.H. Schmeiser, Aristolochic acid as a probable human cancer hazard in herbal remedies: a review, Mutagenesis 17 (2002) 265–277.

[4] J.P. Cosyns, Aristolochic acid and 'Chinese herbs nephropathy': a review of the evidence to date, Drug Saf. 26 (2003) 33–48.

[5] L.S. Gold, T.H. Slone, Aristolochic acid, an herbal carcinogen, sold on the Web after FDA alert, N. Engl. J. Med. 349 (2003) 1576–1577.

[6] J.P. Cosyns, J.P. Dehoux, Y. Guiot, et al., Chronic aristolochic acid toxicity in rabbits: a model of Chinese herbs nephropathy?, Kidney Int 59 (2001) 2164–2173.

[7] Y.J. Wen, L. Qu, X.M. Li, Ischemic injury underlies the pathogenesis of aristolochic acid-induced acute kidney injury, Transl. Res. 152 (2008) 38–46.

[8] J.M. Lee, S. Dedhar, R. Kalluri, et al., The epithelial–mesenchymal transition: new insights in signaling, development, and disease, J. Cell. Biol. 172 (2006) 973–981.

[9] A.A. Pozdzik, I.J. Salmon, F.D. Debelle, et al., Aristolochic acid induces proximal tubule apoptosis and epithelial to mesenchymal transformation, Kidney Int. 73 (2008) 595–607.

[10] M.P. Kalapos, The tandem of free radicals and methylglyoxal, Chem. Biol. Interact. 171 (2008) 251–271.

[11] D.L. Vander Jagt, Methylglyoxal, diabetes mellitus and diabetic complications, Drug Metab. Drug Interact. 23 (2008) 93–124.

[12] R. Meerwaldt, T. Links, C. Zeebregts, et al., The clinical relevance of assessing advanced glycation endproducts accumulation in diabetes, Cardiovasc. Diabetol. 7 (2008) 29.

[13] Y. Lou, J. Li, Y. Lu, et al., Aristolochic acid-induced destruction of organic ion transporters and fatty acid metabolic disorder in the kidney of rats, Toxicol. Lett. 201 (2011) 72–79.

[14] F.Y. Yu, T.S. Wu, T.W. Chen, et al., Aristolochic acid I induced oxidative DNA damage associated with glutathione depletion and ERK1/2 activation in human cells, Toxicol. in Vitro 25 (2011) 810–816.

[15] J.-A. Lee, Y.-C. Tsai, H.-Y. Chen, et al., Fluorimetric determination of d-lactate in urine of normal and diabetic rats by column-switching high-performance liquid chromatography, Anal. Chim. Acta 534 (2005) 185–191.

[16] H. Kaltwasser, H.G. Schlegel, NADH-dependent coupled enzyme assay for urease and other ammonia-producing systems, Anal. Biochem. 16 (1966) 132–138.

[17] D.H. Leaback, P.G. Walker, Studies on glucosaminidase. 4. The fluorimetric assay of N-acetyl-beta-glucosaminidase, Biochem. J. 78 (1961) 151–156.

[18] A. Espinosa-Mansilla, I. Duran-Meras, F.C. Canada, et al., High-performance liquid chromatographic determination of glyoxal and methylglyoxal in urine by prederivatization to lumazinic rings using in serial fast scan fluorimetric and diode array detectors, Anal. Biochem. 371 (2007) 82–91.

[19] C. Gu, H. Qu, L. Han, et al., The effect of raw soybean on oxidative status of digestive organs in mice, Int. J. Mol. Sci. 12 (2011) 8836–8845.

[20] D.Z. Hsu, C.H. Wan, H.F. Hsu, Y.M. Lin, M.Y. Liu, The prophylactic protective effect of sesamol against ferric-nitrilotriacetate-induced acute renal injury in mice, Food Chem. Toxicol. 46 (2008) 2736–2741.

[21] F. Zheng, X. Zhang, Q. Huang, Establishment of model of aristolochic acid-induced chronic renal interstitial fibrosis in rats, Zhonghua Yi Xue Za Zhi 81 (2001) 1095–1100.

[22] F.D. Debelle, J.L. Nortier, E.G. De Prez, C.H. Garbar, A.R. Vienne, I.J. Salmon, M.M. Deschodt-Lanckman, J.L. Vanherweghem, Aristolochic acids induce chronic renal failure with interstitial fibrosis in salt-depleted rats, J. Am. Soc. Nephrol. 13 (2002) 431–436.

[23] C.S. Yang, C.H. Lin, S.H. Chang, et al., Rapidly progressive fibrosing interstitial nephritis associated with Chinese herbal drugs, Am. J. Kidney Dis. 35 (2000) 313–318.

[24] M. Chen, L. Gong, X. Qi, et al., Inhibition of renal NQO1 activity by dicoumarol suppresses nitroreduction of aristolochic acid I and attenuates its nephrotoxicity, Toxicol. Sci. 122 (2011) 288–296.

[25] Y.Y. Chen, J.G. Chung, H.C. Wu, et al., Aristolochic acid suppresses DNA repair and triggers oxidative DNA damage in human kidney proximal tubular cells, Oncol. Rep. 24 (2010) 141–153.

[26] C. Zoccali, F. Mallamaci, G. Tripepi, AGEs and carbonyl stress: potential pathogenetic factors of long-term uraemic complications, Nephrol. Dial. Transplant. 15 (Suppl 2) (2000) 7–11.

[27] N. Bakhiya, V.M. Arlt, A. Bahn, et al., Molecular evidence for an involvement of organic anion transporters (OATs) in aristolochic acid nephropathy, Toxicology 264 (2009) 74–79.

[28] J.L. Vanherweghem, D. Abramowicz, C. Tielemans, et al., Effects of steroids on the progression of renal failure in chronic interstitial renal fibrosis: a pilot study in Chinese herbs nephropathy, Am. J. Kidney Dis. 27 (1996) 209–215.

[29] F.D. Debelle, J.L. Nortier, C.P. Husson, et al., The renin–angiotensin system blockade does not prevent renal interstitial fibrosis induced by aristolochic acids, Kidney Int. 66 (2004) 1815–1825.